Laser joining of different polymer-metal configurations : analysis of mechanical performance and failure mechanisms

E. Rodríguez-Vidal, C. Sanz, J. Lambarri, Jacques Renard, Vladimir Gantchenko

Available online at www.sciencedirect.com

ScienceDirect

Physics Procedia 83 (2016) 1110 – 1117

Physics Procedia

9th International Conference on Photonic Technologies - LANE 2016

Laser joining of different polymer-metal configurations: analysis of mechanical performance and failure mechanisms

E. Rodríguez-Vidal[a,*], C. Sanz[a], J. Lambarri[a], J. Renard[b], V. Gantchenko[b]

[a]*IK4-TEKNIKER, Polo Tecnológico de Eibar, Calle Iñaki Goenaga 5, 20600 Eibar, Guipuzkoa, Spain*
[b]*Centre des Materiaux, Mine de Paris, ParisTech, CNRS UMR 7633 BP 87, 91003 Evry Cedex, France*

Abstract

Direct thermal laser joining of plastic and metallic materials is nowadays arising as an alternative technology for the generation of hybrid joints. The focus of this study is on analyzing the mechanical behavior and failure mechanisms of three polymer-metal configurations: lap, T and Arcan joint configurations. The metal was locally structured by pulsed laser radiation producing micro-patterns to improve adhesion of the polymeric part. Two micro-patterns were considered: low and high distance between pattern centers. Secondly, the opposite side of the micro-structured metal was irradiated by a Continuous Wave (CW) fibre laser to achieve the mechanical interlock between the two materials.

The mechanical performance of lap, T and Arcan joint configurations was assessed by tensile-shear, pull-out and Arcan tests respectively. A comprehensive inspection of the interface was carried out after the mechanical tests. The mechanical performance revealed a meaningful influence of the distance between patterns for the three joint configurations. Furthermore, the Arcan results evidenced a meaningful influence of the angle between the joining plane and the orientation of the applied load. The morphological features of the detached surfaces showed different failure modes depending on the join configuration.

Peer-review under responsibility of the Bayerisches Laserzentrum GmbH

Keywords: polymer-metal hybrid joints; laser joining; laser surface modifications

1. Introduction

The inclusion of non metallic materials such as plastics (plain polymer, copolymers or reinforced polymers) in different industrial fields (automotive, household appliances or aerospace sector) is growing strongly with the main

* Corresponding author. Tel.: +34-943-206-744 .
E-mail address: eva.rodriguez@tekniker.es

Peer-review under responsibility of the Bayerisches Laserzentrum GmbH
doi:10.1016/j.phpro.2016.09.002

aim to reach lightweight structures to slow down energy consumption. However, metals cannot be excluded as fundamental base material from many applications. Thus, most engineering structures or products require multi-components where several types of materials are introduced and the advantages and functionalities of each one are exploited. Metal are normally used to achieve high mechanical properties meanwhile the main advantanges of plastic materials are low weight, high corrosion resistance, and greater design flexibility among others.

Currently there are different robust technologies for use in industry for metal-plastic joining: mechanical joining, mould-in joining and adhesive bonding. In the case of mechanical joining the process requires several careful preparations of the joint and additional assembly elements such as bolts, screws or rivets. Moreover, this technology presents contraints in terms of poor flexibility in joint design. During the moul-in joining the metal part is introduced into the melted polymer during the plastic injection moulding. The main drawback is the hybrid part geometry restriction, given by the mould. Adhesive bonding is a simple and flexible but non-environmentally friendly process that consists in introducing a chemical adhesive in the plastic-metal interfaces. The most important factors limiting the use of adhesive are the environmental degradation of the joints along with the uncertainly forecasting the long-term durability of the joints.

Over the past four years, direct laser joining of plastic and metallic materials has emerged as a promising technology to enable versatile joints free of additional components (adhesive, screws or rivets) (Roesner et al. (2013), Rauschenberger et al. (2015), Jung et al. (2013), Amend et al. (2014)). This process is carried out by two steps. Firstly, the metal part is structured to produce surface irregularities that provide an extra-mechanical interlock with the melted polymer. This pretreatment can be produced by milling (Cenigaonaindia et al. (2012)), plasma torch (Knapp et al. (2014)), grinding (Wahba et al. (2011)) or laser technology (Amend et al. (2014), Heckert et al. (2014)). A greater control of the surface irregularities on a micrometric scale becomes important for hybrid polymer-metal joint considering laser microprocessing. Secondly, during the joining operation, in the case of opaque polymers to the laser wavelength, the laser beam is absorbed on the metal surface and then transferred by conduction to polymer-metal interface. Thus, the melting point of the polymer is achieved and producing the joint after solidication. Several studies have been reported based on the effect of laser structure parameters on the mechanical properties of hybrid polymer-metal joints (Roesner et al. (2011), Amend et al. (2013), Amend et al. (2014), Heckert et al. (2014), Taki et al. (2016) and E. Rodríguez-Vidal et al. (2014)). These researches consider the effect of a wide range of macroscopic, microscopic and nanoscopic patterns produced on the metal surface by different kind of pulsed laser radiation. For the most part, the considered heat source during the joining process was continuous wave laser radiation. The studies cited above analyzed the effect of modifying the metal surface on the hybrid joint's mechanical performance under tensile shear tests. However there has been no investigation focused on the joint's mechanical performance as function of the joint configuration and the stress orientation with respect to the joining plane. The joint configuration and thus the mechanical tests become significant to assess the joint's mechanical performance under the stress conditions of the real application.

The focus of this research is on assessing the effect of three different joint configurations (lap, T and Arcan configurations) on the joint's mechanical performance. Both the microstructuring and joining processes were conducted by laser sources. A brief study about the microstructure conditions was carried out in order to select the suitable texture pattern for the subsequent joining process. The mechanical performance of the different configurations was assessed by tensile-shear, pull-out and Arcan tests for lap, T and Arcan configurations respectively. The effect of the stress orientation is discussed along with the joint's failure mode.

2. Experimental procedure

Materials used in this work were a low alloy steel (HC420LA) and a glass fibre reinforced polyamide (PA6-GF30). In the case of lap and Arcan joint configuration, the samples dimensions were 80x25x0.8mm and 80x25x2.5 for metal and polyamide samples respectively. For T-joint configuration the dimensions were 25x20x0.8mm and 40x25x4mm for metal and polyamide samples respectively.

Metal specimens were microstructured by a nanosecond fibre laser source. Laser movement was produced by a 2D galvo scanning system, capable of scanning structure patterns at high speed. The cross section of the specimens were mounted into Epoxy resin to analyze the depth, width and the recast material height of the produced microstructures by optical microscopy. Ten different measurements of the several microstructure geometric

parameters were carried out for each set of microstructuring conditions, in order to ensure reliable statistics of the results.

Afterward the opposite side of the microstructure metal was irradiated by a CW fibre laser system. Three different joining configurations were considered: lap-joint (Fig. 1a), T-joint (Fig. 1b) and Arcan-joint (Fig. 1c) configurations. During the joining operation, the laser beam heats the metal surface and then the heat is transferred by conduction to the surrounding area, generating the melting of the polymer and producing the joint after solidification. Both materials were clamped in the three configurations by applying a uniform pressure (P=3bar) with a pneumatic clamping device in order to enhance the flow of the molten plastic material into the microstructures of the steel. The joining parameters were laser power P=200W and joining speed v=6mm/s in the case of lap and Arcan-joint configuration and P=74W and v=6mm/s for the T-joints. The considered joining areas were 200, 100 and 700mm^2 for lap, T and Arcan-joint configurations respectively.

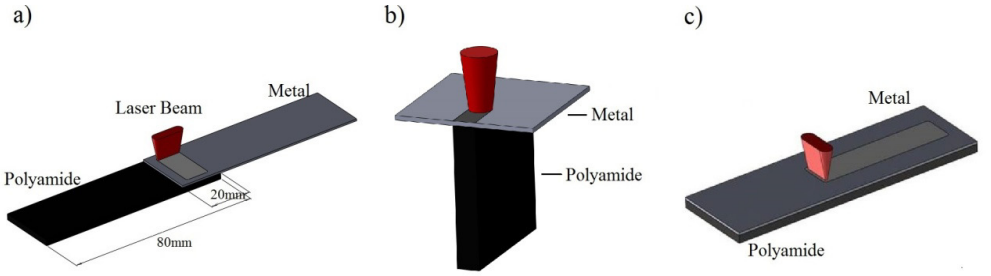

Fig. 1. Scheme of (a) lap; (b) T; (c) Arcan joint configurations.

The mechanical properties of the three different joint-configurations were analyzed by tensile-shear, pull-out and Arcan tests for lap, T and Arcan joint configurations respectively. In the two first cases the joints were analyzed by an Instron 3369 Static Universal machine with a maximum capacity of 50kN and a cross-head displacement of 5mm/mim (Fig. 2a, b). The T-joint samples were mounted in the Instron grips using a tailored clamping device. For each experimental condition, five specimens were tested to ensure the reproducibility of the results. Lastly, the polymer-metal assembly was tested by Arcan-Mines test (Arcan et al. (1987), Joannes et al. (2010)). The hybrid assembly was fixed to the global system by two aluminium anvils (Fig.2c). The tested assembly was located in the middle of a global system described in Fig. 2c). The applied load was orientated at different angles (θ) with respect to the joining plane: from pure shear (θ=0º) to pure tension (θ=90º) including tension and shear mixed mode loading (60º and 30º).

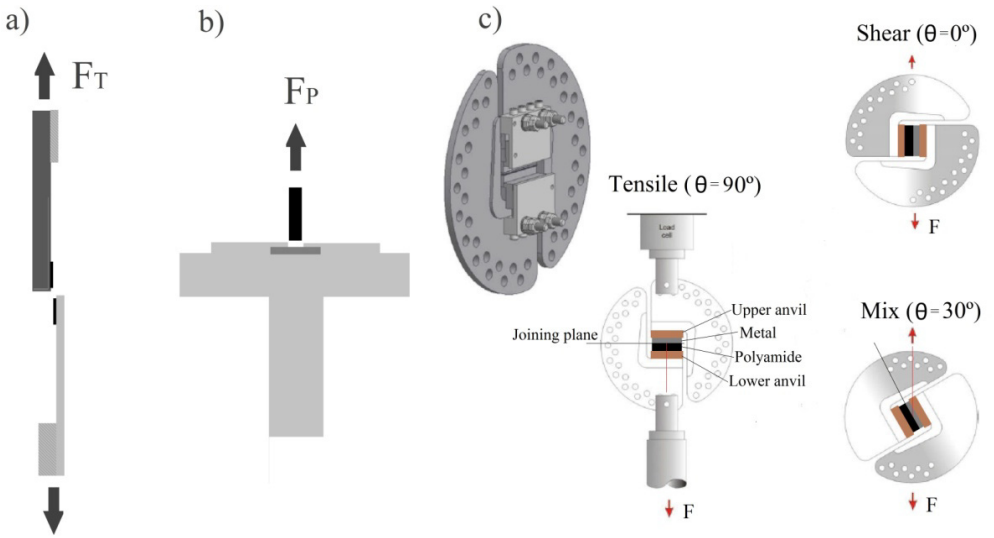

Fig. 2. Scheme of mechanical test for (a) lap; (b) T; (c) Arcan joint configurations.

After mechanical tests a morphological characterization of the detached surfaces (joining interfaces of both metallic and polymer parts) were carried out by Scanning Electron Microscopy (SEM) (Karl Zeiss XB1540) in order to understand the failure mechanisms.

3. Selection of the microstructure pattern.

The microstructure patterns consisted of parallel grooves orientated perpendicularly to the long edge of the plates. The microstructure pattern was defined in terms of groove width (w in Fig. 3), the distance between adjacent grooves ($d_{c\text{-}c}$ in Fig. 3), the groove depth (d in Fig. 3) and the recast material height (h_r in Fig. 3)

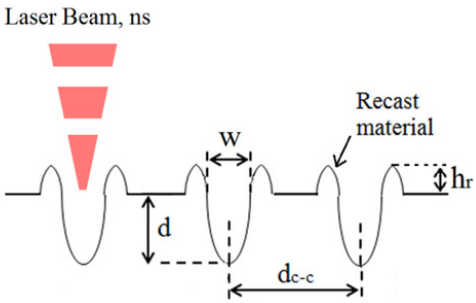

Fig. 3. Schematic relevant microstructure parameters for laser structure produced by nanosecond pulses.

The effect of different groove geometries on tensile-shear mechanical performance was assessed modifying the number of integrations (N_{tracks}). Fig. 4 gathers three representative groove geometries that can be reached ranging the N_{tracks} from 2 to 8. The results reveals a meaningful difference in terms of groove width and depth which involved a significant range of grove aspect ratio values (AR), defined as the ratio of the total depth (h_r+d) to width (w). Table 1 summarizes the groove parameters measured for the three considered geometries. The average groove depth (d) increases when increasing the number of iterations achieving values up to 176µm. Nevertheless, the groove width (w) remains constant for N_{tracks}=2 and 4 but decreases significantly for N_{tracks}=8. The ejected material from the cavity contributes to increase the height of the recast material for N_{tracks}=2 and 4. Nevertheless, for N_{tracks}>4 the additional ejected material produced is placed on the groove neck reducing the groove width and thus, significantly increasing its AR.

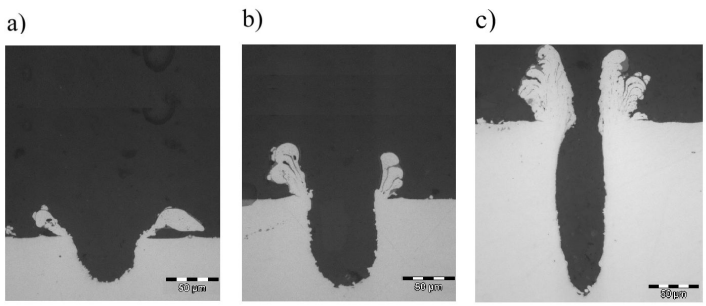

Fig. 4. Cross sections of microstructure on HC420 by nanosecond pulses for (a) N_{tracks}=2; (b) N_{tracks}=4 and (c) N_{tracks}=8.

Table 1. Groove geometry parameters.

N_{tracks}	$\overline{w}[\mu m]$	$\overline{d}[\mu m]$	$\overline{h}_r[\mu m]$	AR	Failure Force $F_T[N]$
2	67 ± 2	43 ± 2	29 ± 4	1.1 ± 0.1	2214 ± 133
4	68 ± 2	82 ± 4	75 ± 3	2.3 ± 0.1	3208 ± 142
8	28 ± 3	176 ± 6	77 ± 5	9 ± 1	Polymer Failure

To select a proper set of microstructure parameters for assessing their effect on different joining configurations, the joining process and the subsequent tensile-shear tests were carried out for the three different groove geometries keeping constant the distance between centers (d_{c-c}=200µm). The mechanical results (Table 1) show an increase of the joint's mechanical performance when the AR increases from 1.1 to 2.3. For AR=9 the failure happened at the polymer and thus, it does not provide information about the joint' s mechanical performance. Since the main objective of this research was focused on assessing the joint's mechanical performance under different configurations, the microstructuring pattern corresponding to N_{tracks}=4 and d_{c-c}=200µm was chosen for the study.

Previous studies (Amend et al. (2013), Amend et al. (2014), Heckert et al. (2014), E.Rodríguez-Vidal et al. (2014), Taki et al. (2015)) examined the impact of different microstructure parameters on the mechanical performance of hybrid joints. They identified the structure density, directly related to the distance between pattern centers, as one of the key parameters. Based on it, the presented study considers two different distance between groove centers for the three joining configurations: d_{c-c}=200, 600µm.

4. Results and discussion

4.1. Mechanical performance

After metal pre-treatment, the specimens were joined and mechanically tested. For each joining configuration the maximum strength was assessed in order to compare the mechanical results. These were evaluated as the ratio of failure force to the corresponding joining area.

Fig. 5a) discloses the strength-strain curves of tensile-shear tests (Fig. 1a) corresponding to two different values of distance between groove centers: d_{c-c}=200 and 600µm. The average maximum strength values were $(\overline{\sigma}_T)_{200} = 16 \pm 1 MPa$ and $(\overline{\sigma}_T)_{600} = 8.6 \pm 0.5 MPa$ for d_{c-c}=200 and 600µm respectively. The results evidence a decrease of about 46% of tensile-shear strength when the distance between groove centers is tripled. The standard deviations associated to the experimental measurement are lower than 7%. In the case of pull-out tests (Fig. 5b) the failure strength values were $(\overline{\sigma}_P)_{200} = 13 \pm 1 MPa$ and $(\overline{\sigma}_P)_{600} = 3.3 \pm 0.5 MPa$ for d_{c-c}=200 and 600µm respectively. In this case the maximum strength was reduced by about 74%. Firstly, the results reveal the same trend for both join configurations. However, a more significant influence of distance between pattern centers is shown in the case of pull-out configuration. For both d_{c-c} values, the joint strength found in the case of tensile-shear performance was significantly higher compared to pull out performance. For tensile-shear strength-strain curves it is possible to notice two different behaviors in the case of d_{c-c}=200 which could be directly related to the randomness of glass fibre orientation within the PA6 matrix. In the case of glass fibre orientation parallel to the applied load the polyamide mechanical properties improve and the strain value for a certain strength is higher than for glass fibre orientated perpendicularly to the applied load.. This effect is not evidenced in the case of pull-out strain curves mainly due to the fact that the maximum failure force achieved was of around 1.4kN, which is significantly lower than the loads accomplished during tensile-shear tests (≈ 3.0kN) and the differences concerning the joining areas.

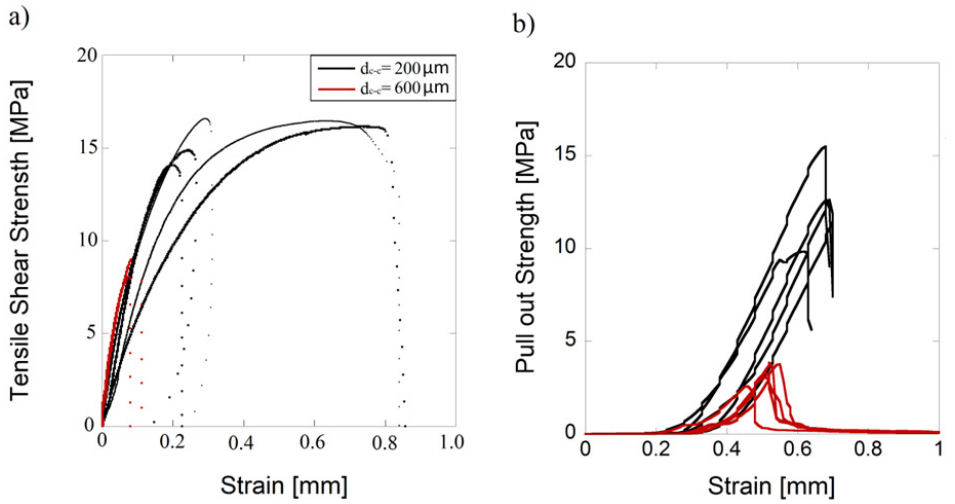

Fig. 5. Mechanical results of (a) tensile-shear tests; (b) pull-out tests for the two structure density values.

Fig. 6a) depicts, as a representative example, the stress-strain curves corresponding to Arcan tests for a distance between groove centers of $d_{c\text{-}c}$=200µm. The results disclose a meaningful influence of the applied load with respect to the joining plane. The failure strength is achieved in the case of pure shear test (Fig. 2c). It is worth to note that the result obtained for pure shear tests ($(\sigma_{\theta=0^\circ})_{200} = 14.6MPa$) falls in the value range found for tensile-shear tests considering the same $d_{c\text{-}c}$ value. The latter means that the tensile-shear tests (Fig.2a), in which the load is not applied exactly on the joining plane, could be recognized as a good approach of pure shear tests for the considered difference of thickness between metal (0.8mm) and polymer (2.5mm). In the case of pure tensile tests (θ=90º) the results obtained from Arcan tests ($(\sigma_{\theta=90^\circ})_{200} = 6.4MPa$) are smaller than the corresponding to the pull-out tests ($(\bar{\sigma}_P)_{200} = 13 \pm 1MPa$)). It could be due to the difference on joining areas between both joint configurations along with the difference on aspect ratio between the joining width and the sample height (40mm for T and 2.5mm for Arcan configuration). The failure strength reveals an exponential decay when increasing the angle between the applied load and the joining plane. (Fig. 6a). The joint's mechanical performance can worsen to 57% depending on the orientation of the applied load.

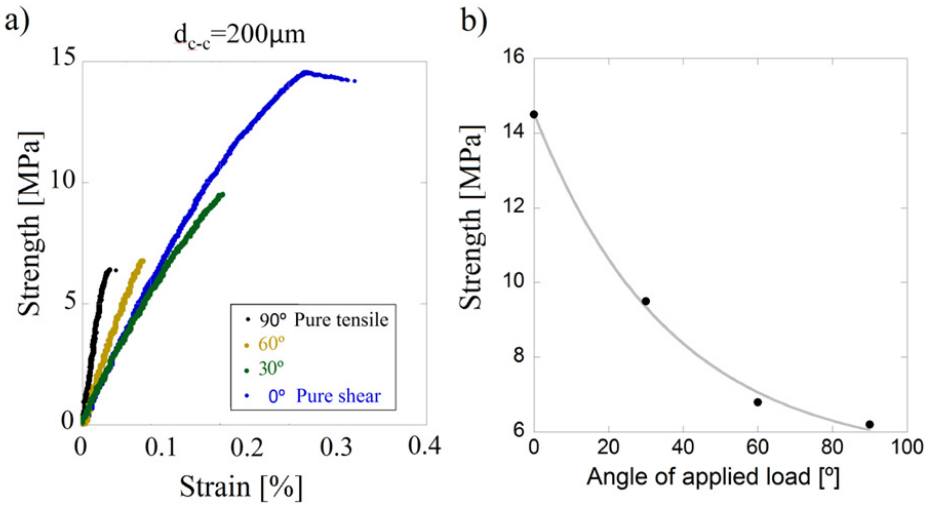

Fig. 6. (a) Stress-Strain curves from Arcan tests for $d_{c\text{-}c}$=200µm; (b) Maximum Strength value as function of the applied load angle for $d_{c\text{-}c}$=200µm.

4.2. Fracture areas

Fig. 7 discloses a top view of the morphological inspection of the detached surfaces (joining interfaces of both metallic and polymer parts) after tensile-shear (Fig.7a) and pull-out tests (Fig.7b) for the considered microstructure conditions: number of iterations of N_{tracks}=4 (Fig.4b) and a distance of groove centers of $_{dc\text{-}c}$=200µm. The metal part corresponding to tensile-shear tests (Fig.7a) evidences the presence of polyamide hooked into the grooves ($1_{t\text{-}s}$). As consequence the polyamide surface does no exhibit a regular pattern since the ridges ($2_{t\text{-}s}$) were partially removed during the mechanical tests. However, the metal surface after pull-out tests (Fig.7b) reveals that there are no traces of polyamide material hooked into the grooves (1_p). The polyamide surface shows a regular imprinted pattern that corresponds to the negative of the microstructure produced on the metal part (E.Rodríguez-Vidal et al. (2015)). In this case a clear ridge (2_p) can be associated to the replication of the groove produced on the metal. Thus, for the same microstructure and joining conditions different failure modes were found depending on the considered joint configuration.

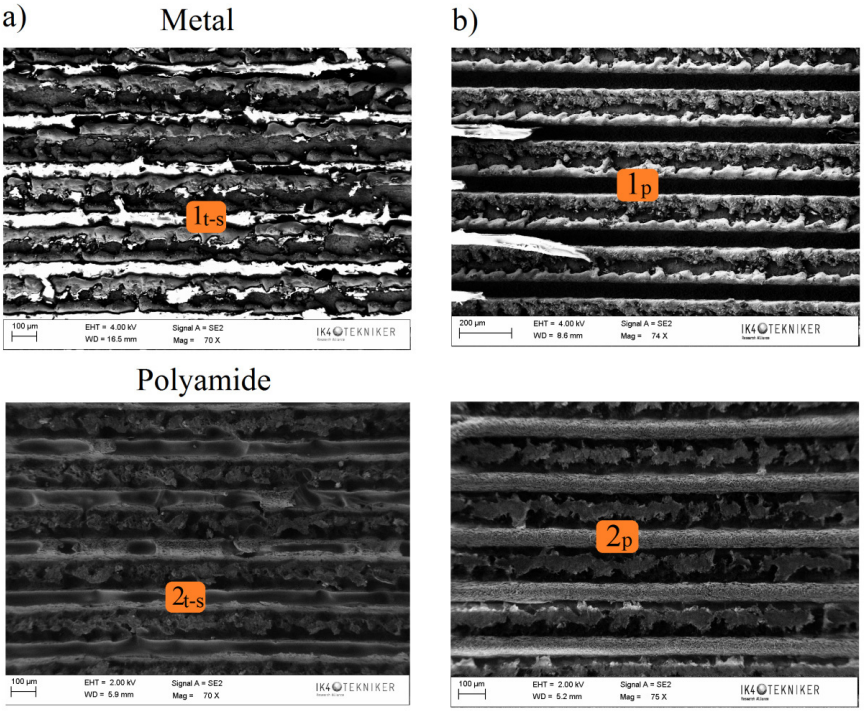

Fig. 7. Top view SEM images of metal and polyamide surfaces after (a) tensile-shear; (b) pull-out tests.

5. Summary and conclusions

Steel surfaces were microstructured by pulsed laser radiation prior to the joining process with a fibre reinforced thermoplastic. The joining process was carried out by CW laser radiation. The effect of different pattern geometries on the joint's tensile-shear performance was assessed to select the more suitable microstructure parameters for the study.

Three different joint configurations were analyzed: lap, T and Arcan joint configurations. Their mechanical performance was evaluated by tensile-shear, pull-out and Arcan tests. For the different joint configurations two different distance between patterns were considered ($d_{c\text{-}c}$=200 and 600µm). The tensile-shear and pull out results revealed the same trend for of mechanical performance as function of $d_{c\text{-}c}$. For the same microstructure conditions, the joints presented worse mechanical properties in the case of T-joint configuration compared to lap-joint

configuration. The achieved results during Arcan tests disclosed a meaningful influence of the angle between the joining plane and the orientation of the applied load. Maximum strength values (≈ 16MPa) were attained for pure shear tests (θ=0º). The strength showed an exponential decay when increasing the mentioned angle, reaching minimum strength values of about 6MPa. The results evidenced the tensile-shear tests as a suitable approach of pure tensile tests for the considered material thicknesses.

The morphological features of the detached surfaces (polymer and metal) after tensile-shear and pull-out tests showed a direct correlation between the failure mode and the obtained maximum strength.

Finally we can conclude that this kind of hybrid plastic-metal joining obtained by laser technology works better under shear loads than pull-out loads getting a stronger interlocking between both materials.

Acknowledgements

The research leading to these results has received funding from the European Union's Seventh Framework Programme (FP7/2007-2013) under grant agreement 309993.

References

Roesner, A., Olowinsky, A., Gillner, A., 2013. Long term stability of laser joined plastic metal parts. Phys. Procedia 41, 169-171.

Rauschenberger, J., Cenigaonaindia, A., Keseberg, J., Vogler, D., Gubler, U., Liébana, F., 2015. Laser hybrid joining of plastic and metal components for lightweight components. Proc. of SPIE 9356, High-Power Laser Materials Processing: Laser, Beam Delivery, Diagnostics and Applications IV.

Jung, K-W., Kawahito, Y., Takahashi, M., Katayama, S., 2013. Laser direct joining of carbon fiber reinforced plastic to aluminum alloy. Journal of Laser Applications 25 (3) 032003.

Amend, P., Mohr, C., Roth, S., 2014. Experimental Investigations of Thermal Joining of Polyamide Aluminum Hybrid using a Combination of Mono- and Polychromatic Radiation. Physics Procedia 56, 824-834. 8th International Conference on Laser Assisted Net Shape Engineering LANE2014

Cenigaonaindia, A., Liebana, F., Lamikiz, A., Echegoyen, Z., 2012. Novel strategies for laser joining of polyamide and AISI 304. Phys. Procedia 39, 92-99. 7th International Conference & Exhibition on Photonic Technologies. LANE2012

Knapp, W., Djomani, D., Coulon, JF., Grunchec, R., 2014. Influence of structuring by laser and plasma torch on the adhesion of metallic films on thermoplastic substrates. Phys. Procedia 56, 791-800. 8th International Conference on Laser Assisted Net Shape Engineering LANE2014.

Wahba, M, Kawahito, Y., Katayama, S., 2011. Laser direct joining of AZ91D thixomolded Mg alloy and amorphous polyethylene terephthalate. Journal of Materials ProcessingTechnology 211, 1166-1174.

Heckert, A., Zaeh, F., 2014. Laser Surface Pre-treatment of Aluminium for Hybrid Joints with Glass Fibre Reinforces Thermoplastics. Physics Procedia 56, 1171-1181. 8th International Conference on Laser Assisted Net Shape Engineering LANE2014.

Roesner, A., Scheik, S., Olowinsky, A., Gillner, A., Poprawe, R., Schleser, M., Reisgen, U., 2011. Innovative Approach of Joining Hybrid Components. Journal of Laser Applications 23, 1-6.

Amend, P., Pfindel, S., Schmidt, M., 2013. Thermal joining of thermoplastic metal hybrids by means of mono- and polychromatic radiation. Physics Procedia 41, 98-105.

Taki, K., Nakamura, S., Takayama, T., Nemoto, A., Ito, H., 2016. Direct joining of a laser-ablated metal surface and polymers by precise injection molding. Microsystem Technologies 22 (1), 31-38.

Rodríguez-Vidal, E.,Lambarri, J., Soriano, Sanz, C.., Verhaerghe, G., 2014. A combined experimental and numerical approach to the laser joining of hybrid Polymer - Metal parts. Physic Procedia 56, 835-844.

Arcan, L., Arcan, M., Daniel, I., 1987. Fractography of Modern Engineering Materials: Composites and Metal. ASTM Special Techn. Publ. 948, 41-67.

Joannes, S., Renard, J., Gantchenko, V., 2010. The role of talc particles in a structural adehsive submitted to fatigue loadings. International Journal of. J. Fatigue 32, 66-71.

Rodríguez-Vidal, E., Sanz, C., Soriano, C., Leunda, C., Verhaerghe, G., 2015. Effect of metal microst-structuring on the mechanical behavior of polymer-metal laser T-joitns. Journal of Materials Processing Technology 229, 668-667.